Investigation on the Microstructure and the Electric Property of Poly(propylene)/Chlorinated Poly(propylene)/ Poly(aniline) Composites

Lin Yang, Jinyao Chen, Huilin Li

State Key Laboratory of Polymer Materials Engineering, Polymer Research Institute of Sichuan University, Chengdu, Sichuan 610065, People's Republic of China

Received 15 February 2008; accepted 15 July 2008
DOI 10.1002/app.29039
Published online 17 October 2008 in Wiley InterScience (www.interscience.wiley.com).

ABSTRACT: The article presents results of studies on composites made from poly(propylene) (PP) modified with poly(aniline) (PANI) doped with dodecylbenzene sulfonic acid (DBSA) and chlorinated poly(propylene) (CPP). The volume resistivity of PP/CPP/PANI composites was detected, and the results show that the volume resistivity decreases with increasing CPP content, and there exists a minimum volume resistivity. Effects of CPP on the microstructure and crystalline structure of the PP/CPP/PANI composites and the relationship between the effects and the electric property were carefully analyzed by scanning electron microscope (SEM) and wide angle X-ray diffraction (WAXD). The method that the specimens of SEM are polished is appropriate to investigate the morphology of conducting polymer composites. The obtained results illuminate that the area of conducting parts and insulating parts obtained from the digital analysis of the SEM image is obviously influenced by the CPP content, the parameters of the lamellar-like structure are immediately related to CPP content and denote the dispersion of PANI-DBSA, and the percent crystallinity and mean crystal size of PP are directly correlated with the CPP content. The increasing area of conducting parts, the increasement of layer distance, the decreasement of size and layer number of the lamellar-like structure of PANI-DBSA, and the increasement of the percent crystallinity and mean crystal size of PP are beneficial to the improvement of the conductive property of PP/CPP/PANI composites. © 2008 Wiley Periodicals, Inc. J Appl Polym Sci 111: 988–997, 2009

Key words: chlorinated poly(propylene); composite; poly(aniline); poly(propylene)

INTRODUCTION

Conductive polymers are expected to yield attractive combinations of properties and are getting more and more attention for researchers all over the world. For many years, they have been making use of these polymers for production of electrical materials,[1–3] especially antistatic materials, sensor materials,[4–6] anticorrosive coating,[7–9] and so on. Among conductive polymers, poly(aniline) (PANI) has the best potential to become economically competitive, because of its cheap materials, simple synthetic method, stability in environment,[10] and high electrical conductivity, which can be reversibly controlled by a change in the oxidation state and protonation of the imine nitrogen groups.[11]

Although PANI has many merits, it is very difficult to be processed in usual methods used in conventional polymers because of its strong intermolecular and innermolecular interactions.[12] For these reasons, wide scale industrial application of PANI has been strongly impeded over several years. Many new protonating agents such as sulfonic acids, phosphoric acid esters,[12,13] and phosphoric acids[14] have been introduced in recent years to improve the processability of PANI. To be worthy to be mentioned, it was Cao et al.[15] that first introduced sulfonic acid as a protonating agent and this made PANI possible to be processed in solvent. Other method to improve the processability of PANI was that PANI was blended with thermoplastic polymers because of its poor mechanical properties.[14,16–18] An unique specialty of this method lies in the combination of electric properties of PANI and mechanical properties of thermoplastic polymers.

Although both the two methods mentioned earlier have its own merits, the second method has more advantages than the first one because it does not need great much of solvent, is more convenient to produce, and is more suitable to wide-scale industrial application. In melt processing of PANI, polar

Correspondence to: H. Li (nic7703@scu.edu.cn).
Contract grant sponsor: National Nature Science Foundation of China; contract grant number: 50233010.
Contract grant sponsor: National Basic Research Program of China; contract grant number: 2005CB623800.

TABLE I
Composition of PP/CPP/PANI Composites

Sample code	PP (wt %)	$PANI_{emer}$ (wt %)	DBSA (wt %)	CPP (wt %)	Theoretical degree of protonation
PP/PANI 1	87.23	4.10	7.79	0.88	0.5
PP/PANI 2	83.70	4.10	7.79	4.41	0.5
PP/PANI 3	79.30	4.10	7.79	8.81	0.5
PP/PANI 4	74.89	4.10	7.79	13.22	0.5
PP/PANI 5	70.49	4.10	7.79	17.62	0.5

polymers such as PVC, poly(methyl methacrylate), polystyrene, and cellulose propionate are usually adopted as thermoplastic matrix[16,17]; moreover, the electrical conductivity of the blends reaches the standard of the antistatic materials. However, the blends prepared by nonpolar polymer (such as poly(propylene) (PP)) and PANI are not satisfactory as the antistatic materials. To reach the standard of the antistatic materials, the molar ratio of PANI is very large in the blend. This certainly will weaken the mechanical properties of the blends.

In this article, we report on the possibility of melt processing of PP/CPP/PANI composites, the relationship between the CPP content and the electric property of PP/CPP/PANI composites, the influence of CPP on the morphology and the structure of the PP/CPP/PANI composites, which are carefully analyzed by SEM and WAXD, and the relationship between the variation of the morphology and structure of the PP/CPP/PANI composites and that of electric property of the PP/CPP/PANI composites.

EXPERIMENTAL

Materials

PANI protonated with hydrochloric acid (HCl) was supplied by Chengdu Organic Chemicals (China) and its electrical conductivity was about 1 S/cm.

PP (PPH-XD-045, melt flow index = 3.5 g/10 min) was supplied by PetroChina (China).

Dodecylbenzene sulfonic acid (DBSA) was supplied by Kewei Chemicals (China) and its content was about 96 wt %.

CPP was supplied by Sichuan Weiye Chemicals (China) and its chlorine content was about 31 wt %.

Preparation of composites

PANI protonated with HCl was neutralized with 20 wt % sodium hydroxide (NaOH) aqueous solution for 48 h and then was filtrated and washed with deionized water until that the pH value of percolate was at 6–8. Obtained polyemeraldine base ($PANI_{emer}$) was dried under vacuum. Purified and dried $PANI_{emer}$ was blended with DBSA, and the molar ratio of DBSA to $PANI_{emer}$ was 0.5. The blend was stirred for 48 h in ambient temperature, and then PANI protonated with DBSA (PANI-DBSA) was gained.

The composites of PP/PANI with different CPP contents were prepared on a two-roll mill and then molded into 1-mm plates. Compression molding was carried out in the following conditions: preheated at 180°C for 5 min at low pressure, compressed for 10 min at 13 MPa at the same temperature, and then cooled to ambient temperature with the cooling rate 30°C/min in the mold at 13 MPa. Specimens with the dimensions of 80 × 80 × 1 mm^3 for the test of volume resistivity were got from the 1-mm plates. The blend compositions with their sample codes were listed in Table I.

Measurement of the volume resistivity

The volume resistivity of the composites was detected in high resistance meter (ZC46A) produced by Shanghai precision Scientific Instrument (China). The result of each sample is average of four measurements.

Scanning electron microscope

A JSM 5900 LV scanning electron microscope (SEM) was used to observe the morphology of the PP/CPP/PANI composites. The specimens were prepared by several methods. The first method is that the specimens are prepared by brittle fracturing under liquid nitrogen and then sputtered with a very thin gold layer [11,19,20]. The second method is that the specimens are prepared by brittle fracturing under liquid nitrogen and are not sputtered with a thin gold layer. The third method is that the specimens are cut from the 1-mm plates with a very sharp knife. The fourth method is that the specimens are cut from the 1-mm plates with a very sharp knife and then polished by a special polisher. With the technique, which the samples of SEM were not sputtered with a thin conducting layer, it was possible to show a contrast between electrically conductive and insulating parts of the material. The SEM photos of nonsputtered samples are not based on a real material contrast, but result from a contrast in

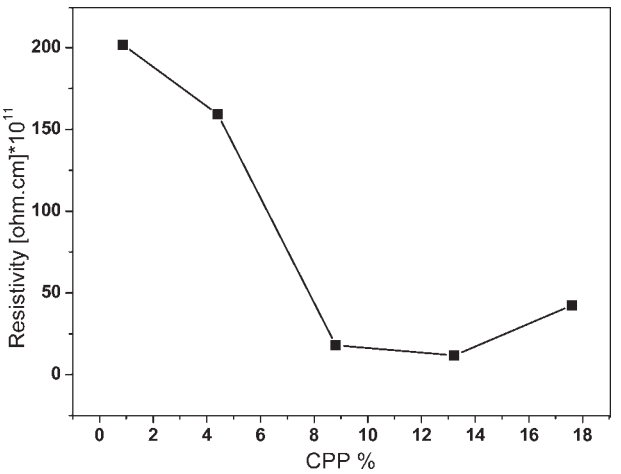

Figure 1 The relation between the volume resistivity and CPP content.

the electrical conductivity between electrically conductive fillers and insulating matrix.[21]

Wide angle X-ray diffraction

Wide angle X-ray diffraction (WAXD) investigations were carried out with a DX-2500 SSC diffractometer (made in China) in the reflection mode. CuKα radiation was used at 40 kV and 25 mA. Investigations were performed in two methods. First, in the range of angles 2°–5°, the scan step was 0.03° (in 2θ) with a counting time of 4 s per step. Second, in the range of angles 5°–45°, the scan step was 0.06° (in 2θ) with a counting time of 2 s per step.

To determine the mass fraction of crystallinity, WAXD curves were deconvoluted into crystalline and amorphous scattering components using the profile fitting program JADE6.5. Each peak was modeled using a Gaussian-Cauchy peak shape. The level of crystallinity was taken as the area ratio of all the crystalline peaks to that of total scattering. The WAXD patterns were also used to evaluate the mean sizes of crystallites. The crystallite size was estimated for planes of PP by using the Scherrer equation

$$D = K\lambda/\beta\cos\theta$$

where D is the crystallite size in the direction perpendicular to the plane, β is the full width at half maximum, $\lambda = 0.154$ nm the wavelength, and θ is the Bragg angle (half of the scattering angle).[14] In this study, the value 0.89 was tentatively used for K.

RESULTS AND DISCUSSION

The volume resistivity of the PP/CPP/PANI composites

The relation between the volume resistivity and CPP content is shown in Figure 1. There exists an interesting phenomenon that the volume resistivity first decreases with increasing CPP content and reaches a minimum volume resistivity when the CPP content is lower than 13.22%, and then increases with further increase of the CPP content. In other words, there exists a minimum volume resistivity among all the composites. CPP is adopted as a compatibilizer and improves the dispersion of PANI-DBSA in the PP/CPP/PANI composites. These are beneficial to decrease the volume resistivity of the PP/CPP/PANI composites.

Morphology of the composites

Figures 2–5 show the SEM micrographs of PP/PANI 3 samples prepared by different methods. Figure 2 shows the SEM image of PP/PANI 3 composite with

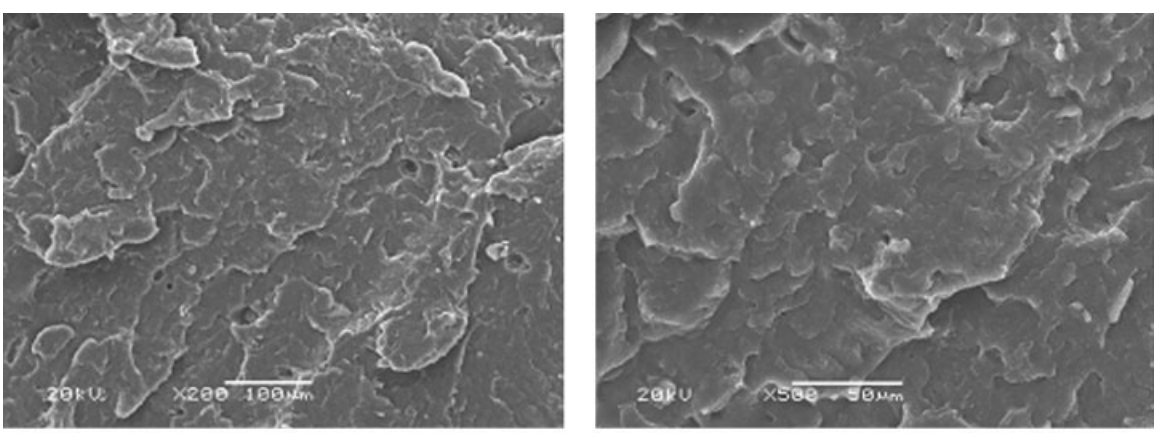

Figure 2 SEM micrographs of PP/PANI 3 composite with the first method.

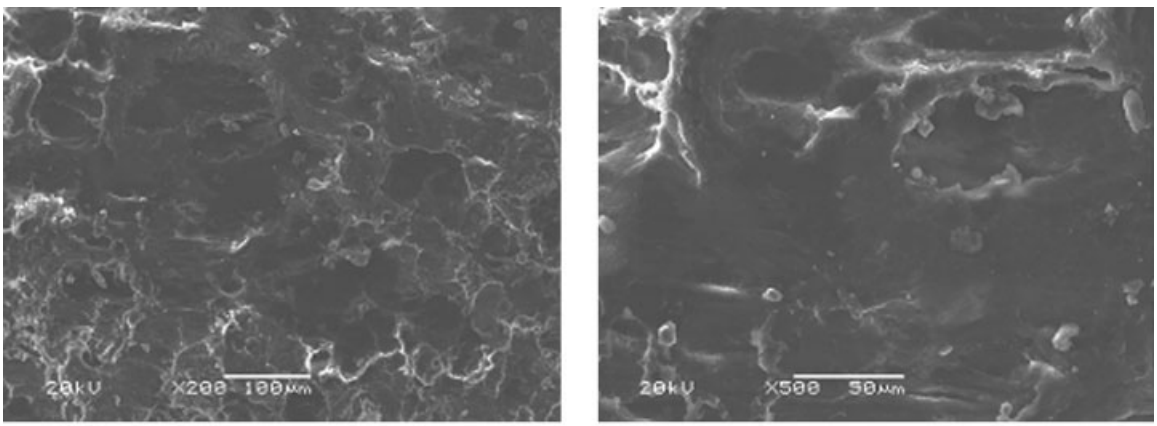

Figure 3 SEM micrographs of PP/PANI 3 composite with the second method.

the first method, which is generally adopted to investigate the morphology of conducting polymer composites. As shown in Figure 2, the phase of dispersion (i.e., the PANI in this study) cannot be clearly separated from the continuous phase (i.e., the PP in this study). The white stripe shown in Figure 2 is only the fracture trace of the specimens. Hence, the number of the white stripe cannot illuminate the property of the PANIs dispersion in the PP/CPP/PANI composite.

Figure 3 shows the SEM image of PP/PANI 3 composite with the second method. The white parts shown in Figure 3 are formed by the accumulative electron. Because the specimens are prepared by brittle fracturing under liquid nitrogen, there exist protuberant parts and concave parts. Consequently, all the pixels shown in Figure 3 do not lie in the same plane. Electron is prone to accumulate in protuberant and insulating parts. Hence, the white parts cannot be definitely ascribed to protuberant parts or insulating parts, the black parts cannot be definitely attributed to conducting parts, and the property of the PANIs dispersion in the PP/CPP/PANI composite cannot be clearly illuminated in this method.

Figure 4 shows the SEM image of PP/PANI 3 composite with the third method. The problem of Figure 4 is analogous to that of Figure 3. All the pixels in Figure 4 do not lie in the same plane, and the property of the PANIs dispersion in the PP/CPP/PANI composite cannot be clearly illustrated in this method.

Figure 5 shows the SEM image of PP/PANI 3 composite with the fourth method. Because, before the SEM observation, the specimens are polished by a special polisher, almost all the pixels shown in Figure 5 lie in the same plane and there are no protuberant parts. Hence, the white parts can be definitely ascribed to insulating parts (i.e., there does not exist

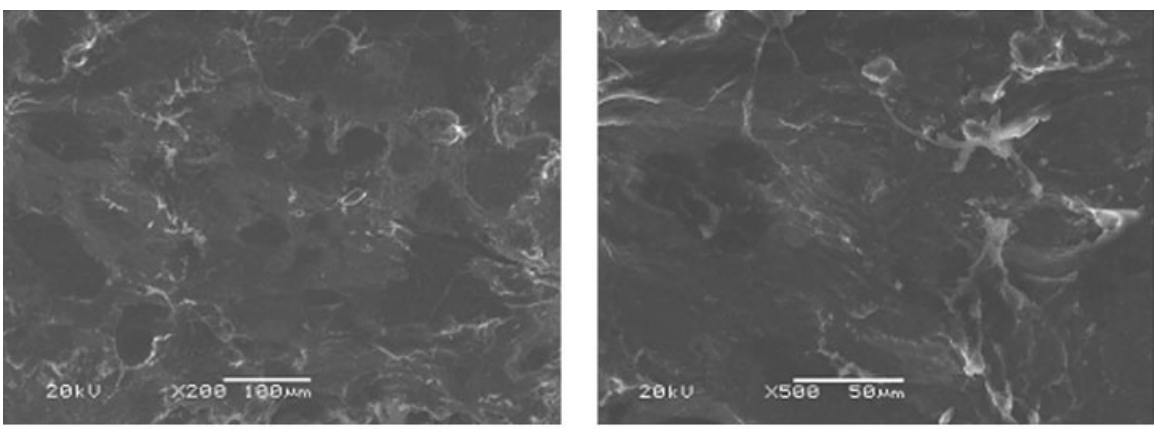

Figure 4 SEM micrographs of PP/PANI 3 composite with the third method.

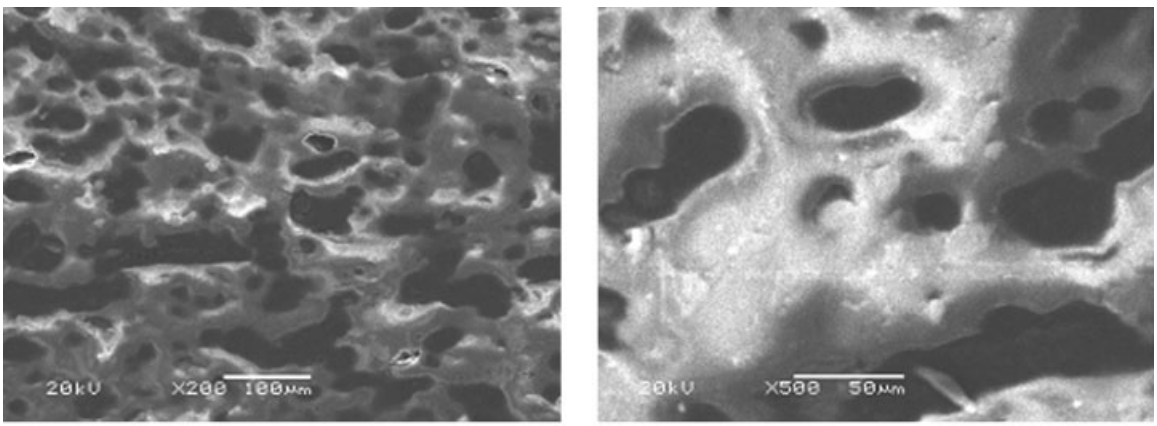

Figure 5 SEM micrographs of PP/PANI 3 composite with the fourth method.

any of PANI.), and the black parts can be clearly ascribed to conducting parts. The gray parts are transition from insulating parts to conducting parts. PANI is also dispersed in the gray parts. The PANI content in the gray parts is lower than that in the black parts and darker is the color, higher is the PANI content. Similarly, this phenomenon of transition exists in transmission electron microscopy (TEM) micrograph of PANI composites in the references.[18,22] Therefore, PANI is dispersed in the gray and black parts, and the property of the PANIs dispersion in the PP/CPP/PANI composite can be elucidated in the fourth method.

Figure 6 shows the SEM micrographs of PP/CPP/PANI composites with the magnification of 200 times whose specimens are prepared by the fourth method. With low CPP content, the continuity of PANI is bad and prone to be interdicted by PP. This makes the ability of conducting electron lower. Hence, the volume resistivity of the PP/CPP/PANI composite is high. With increasing CPP content, the continuity of PANI is intensified, the ability of conducting electron increases, and the volume resistivity of the PP/CPP/PANI composite decreases. With the 13.22% CPP content (i.e., PP/PANI 4), the continuity of PANI is the best, and the dispersion of PANI is the most uniform among all the PP/CPP/PANI composites listed in the Table I. With further increase of the CPP content, the continuity and the dispersion of PANI become worse.

If the intensity of white is defined 255 and that of black is defined 0, and then the range of the color intensity is defined from 0 to 255 in the SEM image, Figure 6 can be digitally analyzed. The area of the range of the color intensity can be statistical. Although there exist some parts to be gray in the range of intensity 150–255, the ability of conducting electron of these gray parts is very weak. Hence, to be statistical conveniently, the range of intensity 0–135 may be regarded as the conducting parts, and the range of intensity 150–255 may be treated as the insulating parts. The color intensity in the range of 135–150 is very difficult to be attributed to the conducting parts or the insulating parts and does not alter the trend of the area of the conducting or insulating parts changed with CPP content. The area of each sample is average of three images.

Figure 7 reveals the trend of the area of the conducting parts and the volume resistivity changed with CPP content. The trendline of the area of the conducting parts versus the CPP content is just contrary to that of the volume resistivity changed with CPP content. The area of the conducting parts first increases with increasing CPP content and reaches a maximum area when the CPP content is lower than 13.22%, and then decreases with further increase of the CPP content. In other words, there exists a maximum area among all the composites. These may illuminate that the volume resistivity is seriously influenced by the area of the conducting parts (i.e., the more area of the conducting parts, the lower volume resistivity).

Figure 8 reveals the trend of the area of the insulating parts and the volume resistivity changed with CPP content. The trend of the area of the insulating parts changed with CPP content is extraordinarily analogous to that of the volume resistivity changed with CPP content. The area of the insulating parts first decreases with increasing CPP content and reaches a minimum area when the CPP content is lower than 13.22%, and then increases with further increase of the CPP content. In other words, there exists a minimum area among all the composites. These may illuminate that the volume resistivity is directly influenced by the area of the insulating parts (i.e., the more area of the insulating parts, the higher volume resistivity).

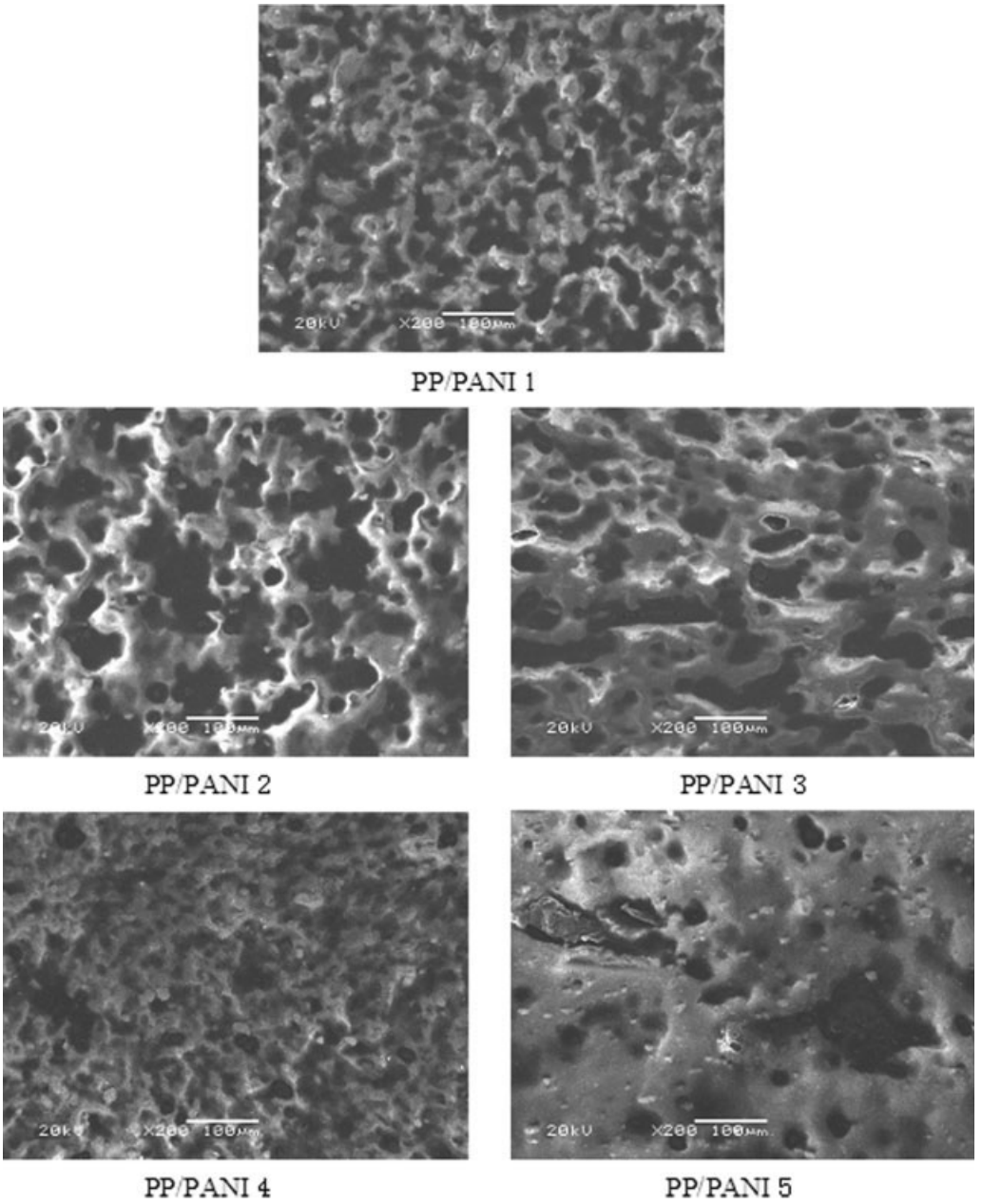

Figure 6 SEM micrographs of PP/CPP/PANI composites with the fourth method.

Wide angle X-ray diffraction study

The lamellar-like structure of PANI

Figure 9 shows the WAXD patterns of the PP/CPP/PANI composites in the range of 2°–5°. The WAXD curves were obtained in the first method. The peak at about 3° is attributed to the lamellar-like structure of PANI-DBSA,[18,23,24] and the lamellar-like structure is also observed in TEM micrograph.[18] The peak at about 3° is distinctly influenced by the CPP content. When the CPP content is lower than 8.81%, there is only one peak at about 3°, and after the CPP content reaches 8.81%, there exist two peaks: one is at about 3°; another small peak is at about 2.6°. These mean that the layer distance of PANI-DBSA increases, the dispersion of PANI improves and the aggregating domains of PANI decreases and becomes loose with increasing CPP content. This is agreeable with the SEM measurement.

To quantify the influence of CPP content on the lamellar-like structural parameter of PANI-DBSA in the PP/CPP/PANI composites, WAXD curves in Figure 9 were fitted using the profile fitting program JADE6.5. A typical example of the profile fitting figure is displayed in Figure 10. The profile fitting results for WAXD curves in Figure 9 are listed in Table II.

The data listed in Table II show the profile fitting results for WAXD curves. XS is the lamellar-like

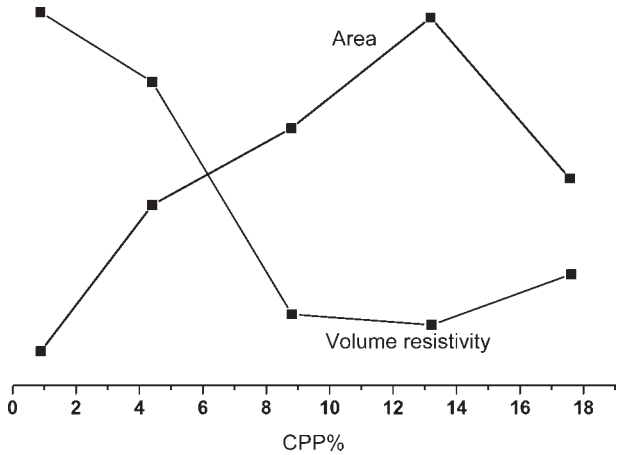

Figure 7 The relationship between the area of the conducting parts and the volume resistivity and CPP content.

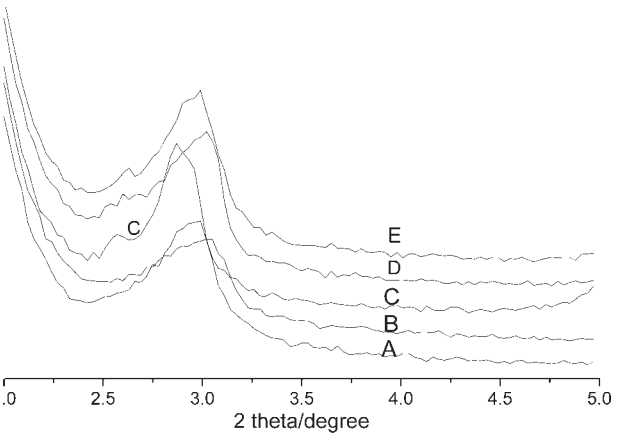

Figure 9 WAXD patterns of (A) PP/PANI 1, (B) PP/PANI 2, (C) PP/PANI 3, (D) PP/PANI 4, and (E) PP/PANI 5 in the range of 2°–5°.

structure size in the direction perpendicular to the plane, and LN is the number of layer in the lamellar-like structure and is obtained from the equation

$$\mathrm{LN} = \mathrm{XS}/d$$

Peak 1 is irrelevant to the lamellar-like structure as it is aroused by air. When the CPP content is lower than 8.81%, with increasing CPP content, the layer distance is not almost changed, but the size of the lamellar-like structure and the number of layer decrease slightly. These may illuminate why the decreasement of the volume resistivity is a little with increasing CPP content when CPP content is lower than 8.81%. After the CPP content reaches 8.81%, there appears another peak at about 2.6° and its layer distance is about 34 Å. These may illuminate why the decreasement of the volume resistivity is very large from PP/PANI 2 to PP/PANI 3. After the CPP content reaches 8.81%, with further increase of the CPP content, two kinds of layer distance are not almost changed; however, two kinds of the size of the lamellar-like structure and the number of layer decrease, and there exist a minimum size of the lamellar-like structure and a minimum number of layers at PP/PANI 4. These may explain why the volume resistivity of PP/PANI 4 is the minimum among all the PP/CPP/PANI composites listed in the Table I.

The reason for the lamellar-like structural parameter changed with the CPP content may be that CPP is inserted into the interlayer of PANI-DBSA layers because of the formation of intermolecular hydrogen bond between CPP and PANI-DBSA, which is proved by FTIR measurement. Hence, the intensity and the number of the intermolecular hydrogen bond directly influence the CPP content inserted into the interlayer of PANI-DBSA layers, which influence the parameter of the lamellar-like structure. The results related FTIR measurement will be published on other journal.

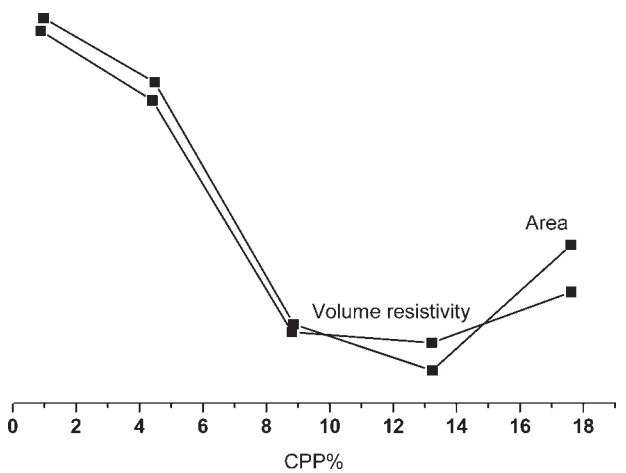

Figure 8 The relationship between the area of the insulating parts and the volume resistivity and CPP content.

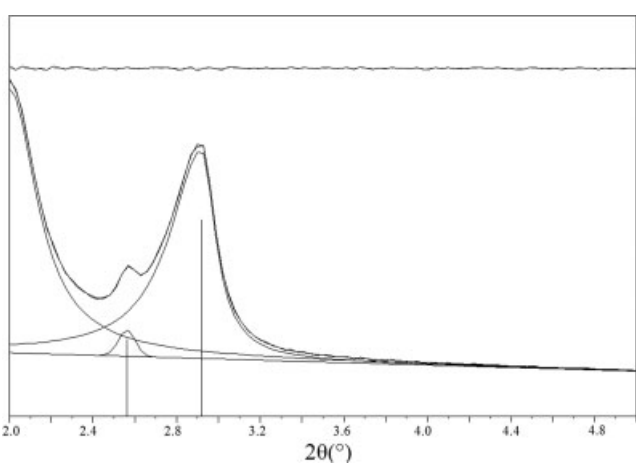

Figure 10 Example of profile fitting of WAXD pattern of PP/PANI 3 in the range of 2°–5°.

TABLE II
Profile Fitting Results for WAXD Curves of PP/CPP/PANI Composites in the Range of 2°–5°

	Peak 1	Peak 2					Peak 3				
Sample code	$2\theta_1$ (°)	$2\theta_2$ (°)	d (Å)	FWHM	XS (Å)	LN	$2\theta_3$ (°)	d (Å)	FWHM	XS (Å)	LN
PP/PANI 1	2.0	2.973	29.69	0.354	234	7.9					
PP/PANI 2	2.0	3.041	29.03	0.406	202	7					
PP/PANI 3	2.0	2.908	30.36	0.256	337	11.1	2.567	34.39	0.108	1000	29.1
PP/PANI 4	2.0	3.039	29.05	0.351	236	8.1	2.595	34.02	0.167	593	17.4
PP/PANI 5	2.0	2.984	29.59	0.338	246	8.3	2.626	33.62	0.141	796	23.7

The crystalline structure

Figure 11 shows the WAXD patterns of the PP/CPP/PANI composites in the range of 5°–45°. The WAXD curves were obtained in the second method. PP is crystallizable and has three kinds of crystalline phases: α-crystal, β-crystal, and γ-crystal. In Figure 11, there exist α-crystal and β-crystal because crystalline peaks at about 14°, 17°, 18.5°, 21° and 21.8° are attributed to α-crystal and crystalline peak at about 16° is attributed to β-crystal.[25] The reason for the formation of β-crystal in the PP/CPP/PANI composites may be that PANI-DBSA acts as β-crystal nucleating agent because there is no β-crystal in PP/CPP composite (the WAXD pattern of the PP/CPP composite is shown in Fig. 12).

To quantify the influence of CPP content on the crystal structure of PP in the PP/CPP/PANI composites, WAXD curves in Figure 11 were fitted using the profile fitting program JADE6.5. The fitting range was chosen at 9°–26° because the crystalline peaks are almost in this range. Using Scherrer's law and the mass fraction of crystal formula (e.g., % crystallinity $= A_c/(A_c + A_n)$, where A_c is the scattering from sharp crystalline area peaks and A_n is the scattering from noncrystalline areas), the crystal size corresponding to peaks and the percent crystallinity of the PP/CPP/PANI composites were calculated. A typical example of the profile fitting figure is displayed in Figure 13. The profile fitting results of WAXD curves in Figure 11 are listed in Table III.

The data listed in Table III show the profile fitting results of WAXD curves. Although the interplanar distance of α-crystal and β-crystal does not change very distinctly with the CPP content, there exists some disciplinary diversification. All the interplanar distance first increase with increasing CPP content and reach a maximum interplanar distance when the CPP content is lower than 13.22%, and then decrease with further increase of the CPP content. In other words, there exists a maximum interplanar distance among all the composites. The percent crystallinity of the PP/CPP/PANI composites first increases with increasing CPP content and reaches a maximum percent crystallinity when the CPP content is lower than 4.41%, and then decreases with further increase of the CPP content. However, the percent crystallinity of the PP/CPP/PANI composites is only an apparent percent crystallinity and cannot reflect the actual percent crystallinity of PP in the PP/CPP/PANI composites as A_n includes three kinds of noncrystalline area (PP, CPP, and PANI-DBSA). Each kind of noncrystalline area is very difficult to be obtained. Hence, a simple method is adopted to obtain the relative percent crystallinity of PP. The method is that the relative percent crystallinity is obtained from the equation

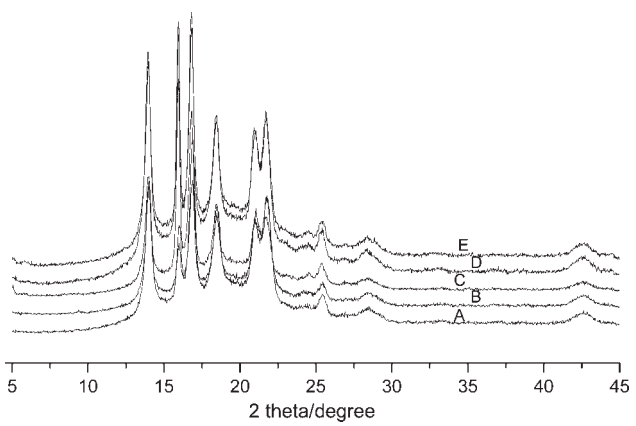

Figure 11 WAXD patterns of (A) PP/PANI 1, (B) PP/PANI 2, (C) PP/PANI 3, (D) PP/PANI 4, and (E) PP/PANI 5 in the range of 5°–45°.

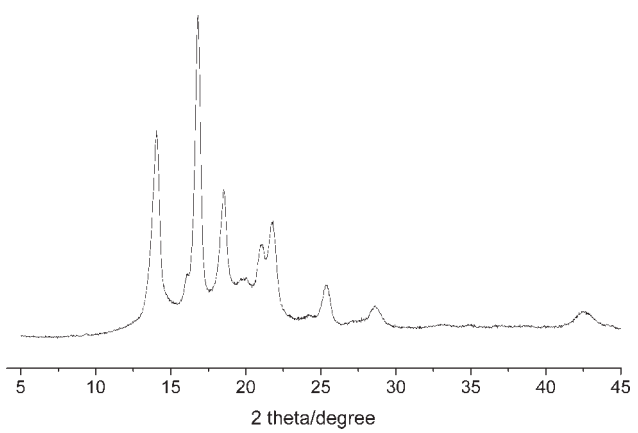

Figure 12 WAXD pattern of the PP/CPP composite.

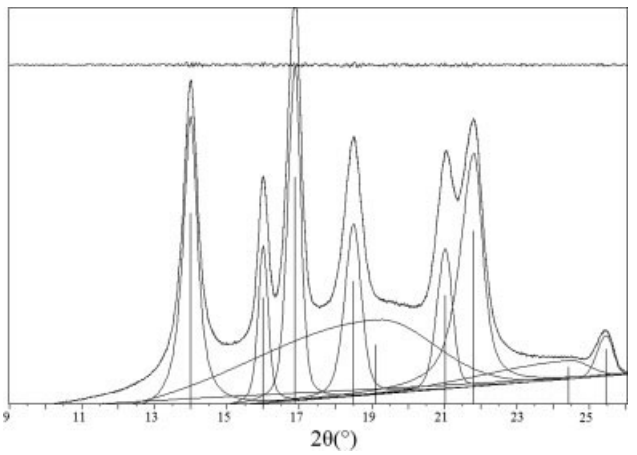

Figure 13 Example of profile fitting of WAXD pattern of PP/PANI 1 the range of 9°–26°.

$$\text{Relative crystallinity \%} = \text{Crystallinity \%/PP \%}$$

The results of relative crystallinity are listed in Table IV. To evaluate the influence of CPP content on the size of crystallite, mean size of crystallite is introduced, because effect of CPP content on crystal size of each peak is different and it is not reasonable to choose any crystal size to represent the size of crystallite. Mean size of crystallite is obtained from the equation

$$\text{Mean size of crystallite} = (XS_{A1} + XS_B + XS_{A2} + XS_{A3} + XS_{A4} + XS_{A5})/6$$

The results of mean size of crystallite are listed in Table IV.

Figure 14 shows plots of volume resistivity, relative crystallinity, and mean size of crystallite versus CPP content. The relative crystallinity first increases with increasing CPP content when the CPP content is lower than 8.81%, and then does not increase with further increase of the CPP content. The reason of this phenomenon may be that although CPP is not crystallizable, it may be an inducement, which makes PP be prone to crystallize. When the CPP content is superabundant, the action of inducement will be limited. The trend of relative crystallinity changed with the CPP content is analogous to that of the volume resistivity changed with the CPP content. This phenomenon also appears in the PANI-HCSA/nylon 6 blends[26] and is contrary to the reference.[14] The mean size of crystallite first increases with increasing CPP content when the CPP content is lower than 8.81%, and then does not increase with further increase of the

TABLE III
Structural Parameters for PP/CPP/PANI Composites by Means of WAXD

Sample code	Crystallinity (%)		2θ (°)	*d* (Å)	FWHM	XS (Å)
PP/PANI 1	52.64	A1	14.0	6.321	0.469	176
		B	16.0	5.537	0.32	268
		A2	16.9	5.251	0.421	198
		A3	18.49	4.796	0.534	154
		A4	21.03	4.222	0.633	129
		A5	21.78	4.078	0.562	146
PP/PANI 2	61.06	A1	13.99	6.324	0.44	189
		B	15.99	5.538	0.296	293
		A2	16.86	5.255	0.392	214
		A3	18.45	4.805	0.529	155
		A4	20.96	4.236	0.906	90
		A5	21.77	4.079	0.491	169
PP/PANI 3	59.44	A1	13.98	6.329	0.419	199
		B	15.94	5.554	0.241	376
		A2	16.81	5.270	0.371	227
		A3	18.45	4.806	0.452	184
		A4	20.97	4.232	0.496	167
		A5	21.75	4.084	0.559	147
PP/PANI 4	56.06	A1	13.96	6.341	0.421	198
		B	15.95	5.554	0.245	370
		A2	16.81	5.270	0.365	231
		A3	18.42	4.812	0.488	169
		A4	20.94	4.240	0.557	148
		A5	21.71	4.090	0.545	151
PP/PANI 5	53.40	A1	13.98	6.331	0.415	201
		B	15.95	5.553	0.231	397
		A2	16.81	5.269	0.349	243
		A3	18.45	4.806	0.457	181
		A4	21.00	4.228	0.525	157
		A5	21.74	4.085	0.545	151

TABLE IV
Calculating Results

Sample code	Relative crystallinity (%)	Crystallinity (%)	Mean size of crystallite (Å)	PP (%)
PP/PANI 1	62.74	52.64	178.5	83.90
PP/PANI 2	73.11	61.06	185	83.52
PP/PANI 3	75.13	59.44	216.7	79.12
PP/PANI 4	75.02	56.06	211.2	74.73
PP/PANI 5	75.93	53.40	221.7	70.33

CPP content. The trend of mean size of crystallite changed with the CPP content is analogous to that of the volume resistivity shifted with the CPP content. In accordance with these observations, the formation of big crystallite and high relative crystallinity of a host polymer are favor to decrease the volume resistivity, probably because of the better formation of conductive pathways, which are engendered by conductive PANI as a consequence of the exclusion of PANI into interspherulitic domains due to the crystallization of PP.

CONCLUSIONS

In this article, the volume resistivity of the PP/CPP/PANI composites was detected. SEM and WAXD were adopted to analyze the effect of CPP content on the morphology and structure of the composites. The obtained results allow for the formulation of the following conclusions:

1. The method that before the SEM observation, the specimens are polished by a special polisher is appropriate to investigate the morphology of conducting polymer composites. The area of conducting parts and insulating parts obtained from the digital analysis of the SEM image is obviously influenced by the CPP content. Furthermore, the volume resistivity of composite is seriously influenced by the area of conducting parts and insulating parts.

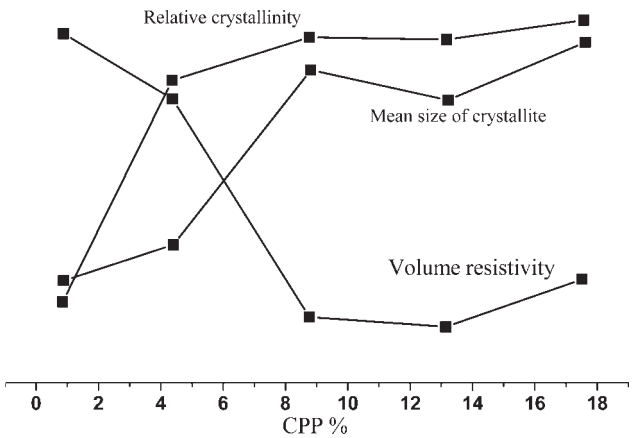

Figure 14 Volume resistivity, relative crystallinity, and mean sizes of crystallites versus CPP content.

2. The layer distance and the size of the lamellar-like structure and the number of layer are closely related to CPP content, denote the dispersion of PANI-DBSA in PP/CPP/PANI composites, and immediately influence the volume resistivity of composites.
3. The percent crystallinity and mean crystal size of PP are directly influenced by the CPP content and are correlated with the formation of conductive pathways of PANI-DBSA in the PP/CPP/PANI composites.

References

1. Shirakawa, H. Synth Met 2001, 125, 3.
2. MacDiarmid, A. G. Synth Met 2001, 125, 11.
3. Heeger, A. J. Synth Met 2001, 125, 23.
4. Koul, S.; Chandra, R.; Dhawan, S. K. Sens Actuators B 2001, 75, 151.
5. Gerard, M.; Chaubey, A.; Malhotra, B. D. Biosens Bioelectron 2002, 17, 345.
6. Jin, Z.; Su, Y.; Duan, Y. Sens Actuators B 2000, 71, 118.
7. Bernard, M. C.; Hugot-Le Goff, A.; Joiret, S.; Phong, P. V. Synth Met 2001, 119, 283.
8. Mirmohseni, A.; Oladegaragoze, A. Synth Met 2000, 114, 105.
9. Araujo, W. S.; Margarit, I. C. P.; Ferreira, M.; Mattos, O. R.; Lima Neto, P. Electrochim Acta 2001, 49, 1307.
10. MacDiarmid, A. G. Synth Met 1997, 84, 27.
11. Barra, G. M. O.; Leyva, M. E.; Soares, B. G.; Mattoso, L. H.; Sens, M. J Appl Polym Sci 2001, 82, 114.
12. Luzny, W.; Kaniowski, T.; Pron, A. Polymer 1998, 39, 475.
13. Pron, A.; Luzny, W. Laska, J. Synth Met 1996, 80, 191.
14. Fryczkowski, R.; Slusarczyk, C.; Fabia, J. Synth Met 2006, 156, 310.
15. Cao, Y.; Smith, P.; Heeger, A. J. Synth Met 1992, 48, 91.
16. Laska, J.; Zak, K.; Pron, A. Synth Met 1997, 84, 117.
17. Laska, J.; Pron, A.; Zagorska, M.; Lapkowski, S.; Lefrant, S. Synth Met 1995, 69, 113.
18. Passiniemi, P.; Laakso, J.; Osterholm, H.; Pohl, M. Synth Met 1997, 84, 775.
19. Ho, K. S.; Hsieh, K. H.; Huang, S. K.; Hsieh, T. H. Synth Met 1999, 107, 65.
20. Jia, W.; Tchoudakov, R.; Segal, E.; Joseph, R.; Narkis, M.; Siegmann, A. Synth Met 2003, 132, 269.
21. Taipalus, R.; Harmia, T.; Zhang, M. Q.; Friedrich, K. Compos Sci Technol 2001, 61, 801.
22. Salahuddin, N.; Ayad, M. M.; Ali, M. Polym Adv Technol 2008, 19, 171.
23. Levon, K.; Ho, K. H.; Zheng, W. Y.; Laakso, J.; Kärnä, T.; Taka, T.; Österholm, J. E. Polymer 1995, 36, 2733.
24. Pan, W.; Yang, S. L.; Li, G.; Jiang, J. M. Eur Polym J 2005, 41, 2127.
25. Obadal, M.; Cermak, R.; Stoklasa, K. Macromol Rapid Commun 2005, 26, 1253.
26. Hopkins, A. R.; Reynolds, J. R. Macromolecules 2000, 33, 5221.